Gravity Field Recovery from GRACE-SST Data of Short Arcs

Torsten Mayer-Gürr, Annette Eicker, and Karl Heinz Ilk

Institute of Theoretical Geodesy, University of Bonn, D-53115 Bonn, Germany
tmg@geod.uni-bonn.de

Summary. The signal content in the low-low SST observables of the gravity field twin-satellite mission GRACE (Gravity Recovery And Climate Experiment) varies in the space domain depending on the roughness of the gravity field features. On the one hand, the maximum degree of the spherical harmonic expansion has to be selected as high as possible to bring out the maximum of gravity field information out of the data. On the other hand, an increasing maximal degree deteriorates the stability of the normal equations to solve for the gravity field parameters. Therefore, a trade-off is necessary between the selection of a maximal degree adequate for representing the signal content in the observables, on the one hand, and a maximal degree which can still be recovered without causing instabilities, on the other hand. We propose to integrate the global gravity field recovery with regional gravity field refinements tailored to the specific gravity field features in these regions: In a first step, the gravity field only up to a moderate safely determinable degree is recovered; the specific analysis features tailored to the individual gravity field characteristics in areas of rough gravity field signal will be modelled subsequently by space localizing base functions in a second step. In a final third step, a spherical harmonic expansion up to an (in principle) arbitrary degree can be derived based on a numerical Gauss – Legendre - quadrature procedure without any stability problems. The procedure will be applied in a first example to observations of a GRACE simulation scenario to test the potential capabilities of the approach. A second application demonstrates the determination of a global gravity field model and regional refinements based on low-low SST data of the GRACE twin satellite mission for the August 2003 observations.

Key words: GRACE, SST, low-low, high-low, global gravity field recovery, gravity field refinement, gravity field zoom-in, space localizing base functions, Gauss-Legendre-quadrature

1 Introduction

As a result of the dedicated space-borne gravity field mission GRACE (Gravity Recovery And Climate Experiment – Tapley et al. 2004), in orbit since

2002, a breakthrough in accuracy and resolution of gravity field models has been achieved. Subsequent solutions by using the observations collected over a period of time of, e.g., one month, enables the derivation of time dependencies of the gravity field parameters. The innovative character of this mission lies in the continuous observation of the twin satellites by the Global Positioning System (GPS) and the highly precise line-of-sight range and range-rate K-band measurements between the twin satellites. In addition, the surface forces acting on these satellites are measured and can be considered properly during the recovery procedure. As a result of this mission, the presently best combination static model, EIGEN-CG03C, has been derived from 376 days of GRACE observations and three years of CHAMP (Förste et al., 2005) as well as monthly snap-shots of the gravity field, showing clearly temporal variations of the gravity field closely correlated to the hydrological water cycle. Another GRACE gravity field model is GGM02C, based on the analysis of 363 days of GRACE in-flight data (Centre of Space Research, Austin, - UTEX CSR, 2004, http://www.csr.utexas.edu/grace/gravity). It is represented by a spherical harmonic expansion up to degree 200 and constrained with terrestrial gravity information.

These gravity field models are represented, as usual, in terms of spherical harmonics. A disadvantage of this kind of gravity field modelling is the missing flexibility. Because of the inhomogeneous structure of the gravity field in the space domain the signal to noise ratio varies in the satellite-to-satellite tracking observables depending on the geographical region the satellite is actually passing. The heterogeneity of the gravity field cannot be properly taken into account in case of global solutions based on spherical harmonic expansions. The reason is that the recovery of the gravity field by satellite techniques is an improperly posed problem which requires a proper regularization that influences especially the high frequent spectral part of the gravity field. In most cases, a Tichonov-type regularization is applied which acts globally in case of a gravity field representation by base functions of global support. The regularization parameter can be derived by the L-curve procedure, by cross validation or by a recently proposed method of variance component estimation (Koch and Kusche, 2003; Mayer-Gürr et al., 2005). The establishment of the regularization matrix usually is based on Kaula's rule of thumb or derived from the degree variances of an available gravity field model. The disadvantage of this sort of uniform global regularization is that the regularization factor is selected such that an overall filtering of the observations leads to a mean damping of the global gravity field features. Depending on the procedure for selecting the regularization factor, the consequences are either an over-damping of the rough gravity field features, while the smoother parts would need a slightly stronger regularization to avoid a contamination of the recovery results by observation noise, or vice-versa.

This disadvantageous property suggests a hybrid modelling of the gravity field: the long wavelength features of the gravity field should be represented by a series of spherical harmonics up to a properly selected degree and the

gravity field details should be modelled by series of space localizing base functions such as spherical wavelets or harmonic spline functions. The maximum degree of the spherical harmonic representation has to be selected depending on the measurement scenario; the space localizing gravity field parameters have to be recovered by a regionally adapted recovery procedure and an individual regularization which is tailored to the roughness of the gravity field in specific regions of the Earth. There are various possibilities to adapt the space localizing base functions to the individual gravity field features such as the customization of the resolution properties of the base function to enable an optimal fit to the gravity field spectrum to be recovered and the definition of the nodal point distribution necessary to model the individual gravity field structures properly. It is also very easy to include additional conditions for the regional gravity field solutions, such as inclinations of the geoid in special parts, or more general, arbitrary functionals of the gravity field parameters. Furthermore, several regional solutions with global coverage can be merged to obtain a global solution. A spherical harmonic representation, in principle up to an arbitrary maximum degree and only limited by the maximal signal content of the observations, can be obtained by means of numerical quadrature methods now in a direct stable way avoiding the instable inverse procedure. It should be pointed out that in the approach presented here, the above mentioned disadvantages of a global solution by spherical harmonics, derived by an inversion procedure, are avoided, as demonstrated by Eicker et al. (2005).

The mathematical model of our recovery approach is sketched in Sect. 2. Details to the method as far as the global recovery by spherical harmonics are concerned are presented, e.g., in Mayer-Gürr et al. (2005). In Sect. 3 the combination of normal matrices based on individual short arcs is explained as well as the weighting of the normal matrices within a variance component estimation procedure including the computation of the regularization parameter. In Sect. 4, a simulation scenario is presented and the potential capabilities of the method are demonstrated based on a global gravity field recovery from SST range-rate observations. The solutions of a global gravity field recovery from the GRACE low-low SST data of August 2003 with a global coverage of regional refinement patches are presented in Sect. 5. The results are compared to the gravity field models EIGEN-CG03C and GRACE-GGM02C and demonstrate the high quality in the spectral band above degree n=60 of a spherical harmonic expansion. Sect. 6 contains a summary and an outlook for future investigations.

2 Setup of the mathematical model

The gravity field recovery approach tailored to a twin satellite gravity mission of the GRACE type as presented here, is based on Newton's equation of motion, formulated as a boundary value problem in the form of a Fredholm type integral equation. This idea has been proposed as a general method for orbit

determination by Schneider in 1967 (Schneider, 1968), modified for gravity field determination by Schneider and Reigber (1969), investigated in detail by Reigber (1969) and successfully applied subsequently. In the following, the idea has been applied to the satellite-to-satellite tracking (SST) problem by Ilk (1984) and later to the satellite gravity gradiometry (SGG) analysis. After that, the method has been developed and tested based on various simulation scenarios, e.g. see Ilk et al. (1995). As first real data applications, the gravity field models ITG-CHAMP01 and ITG-CHAMP02 have been derived based on this method, applied to the analysis of kinematical short arcs (Mayer-Gürr et al., 2005). The basic characteristic of this method is the use of short arcs for regional and global gravity field recovery applications. The complete recovery procedure consists of three steps which can be applied independently as well:

- Global gravity field recovery based on a spherical harmonic expansion up to a moderate degree to provide a first global reference model as a basis for further refinements,
- Regional refinements of the gravity field by spherical splines as space localizing base functions, adapted to the specific gravity field features, if possible covering the globe,
- Determination of a global gravity field model by merging the regional refinement solutions and deriving potential coefficients by a numerical quadrature technique.

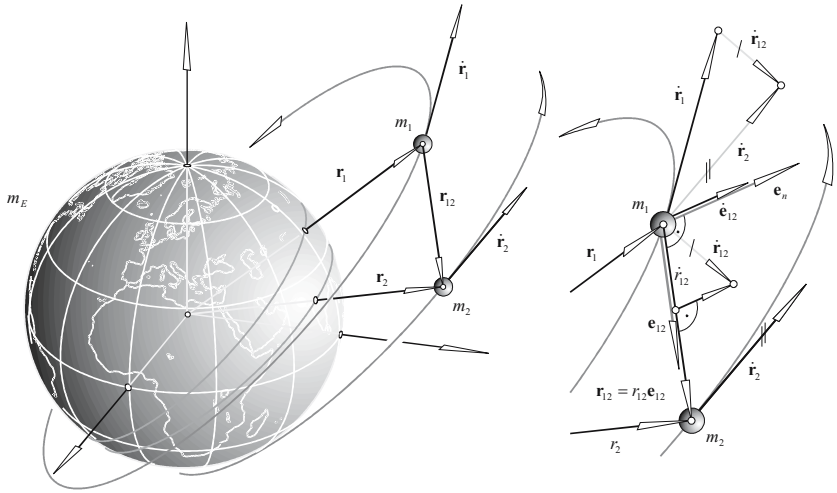

Fig. 1. Low-low satellite-to-satellite tracking experiment

2.1 The equation of relative motion for twin satellites

If precise intersatellite functionals as line-of-sight ranges or range-rate measurements are available, as in case of the GRACE mission, the mathematical model can be based on Newton's equation of motion for the line-of-sight distance (Fig. 1),

$$\ddot{r}_{12}(t) = \frac{\dot{\mathbf{r}}_{12}^2 - \dot{r}_{12}^2}{r_{12}} + \mathbf{e}_{12} \cdot \mathbf{g}(t; \mathbf{r}_{12}, \mathbf{r}_1, \dot{\mathbf{r}}_1, \dot{\mathbf{r}}_2; \mathbf{x}), \tag{1}$$

formulated as a boundary value problem,

$$\begin{aligned} r_{12}(t) = {} & (1-\tau)\, r_{12,A} + \tau r_{12,B} - \\ & - T^2 \int_{\tau'=0}^{1} K(\tau, \tau') \left(\frac{\dot{\mathbf{r}}_{12}^2 - \dot{r}_{12}^2}{r_{12}} + \mathbf{e}_{12} \cdot \mathbf{g}(t; \mathbf{r}_{12}, \mathbf{r}_1, \dot{\mathbf{r}}_1, \dot{\mathbf{r}}_2; \mathbf{x}) \right) d\tau', \end{aligned} \tag{2}$$

satisfying the boundary values,

$$r_{12,A} := r_{12}(t_A), \quad r_{12,B} := r_{12}(t_B), \quad t_A < t_B. \tag{3}$$

The quantity $K(\tau, \tau')$ is the integral kernel,

$$K(\tau, \tau') = \begin{cases} \tau\,(1-\tau'), & \tau \le \tau', \\ \tau'\,(1-\tau), & \tau' \le \tau, \end{cases} \tag{4}$$

with the normalized time variable,

$$\tau = \frac{t - t_A}{T} \quad \text{with} \quad T = t_B - t_A, \quad t \in [t_A, t_B]\,. \tag{5}$$

The solution can be given in spectral form as follows,

$$r_{12}(t) = (1-\tau)\, r_{12,A} + \tau r_{12,B} + \sum_{\nu=1}^{\infty} r_{12,\nu} \sin(\nu \pi \tau)\,, \tag{6}$$

with the coefficients $r_{12,\nu},\ \nu = 1, 2, ..., \infty$,

$$\begin{aligned} r_{12,\nu} = {} & -\frac{2T^2}{\pi^2 \nu^2} \int_{\tau'=0}^{1} \sin(\nu \pi \tau') \cdot \\ & \cdot \left(\frac{\dot{\mathbf{r}}_{12}^2 - \dot{r}_{12}^2}{r_{12}} + \mathbf{e}_{12} \cdot \mathbf{g}(\tau'; \mathbf{r}_{12}, \mathbf{r}_1, \dot{\mathbf{r}}_1, \dot{\mathbf{r}}_2; \mathbf{x}) \right) d\tau'. \end{aligned} \tag{7}$$

The coefficients $\mathbf{r}_\nu,\ \nu = 1, 2, ..., \infty$, of (6) can be derived from the right hand side of (1) (for details see Ilk et al., 1995). The specific force function,

$$\begin{aligned} \mathbf{g}(\tau'; \mathbf{r}_{12}, \mathbf{r}_1, \dot{\mathbf{r}}_1, \dot{\mathbf{r}}_2; \mathbf{x}) = {} & \mathbf{g}_d(\tau'; \mathbf{r}_1, \mathbf{r}_2, \dot{\mathbf{r}}_1, \dot{\mathbf{r}}_2) + \nabla V_{(12)E}(\tau'; \mathbf{r}_{12}, \mathbf{r}_1; \mathbf{x_0}) + \\ & + \nabla T_{(12)E}(\tau'; \mathbf{r}_{12}, \mathbf{r}_1; \Delta\mathbf{x}), \end{aligned} \tag{8}$$

with the gravity field parameters $\mathbf{x}$ can be separated in a disturbance part $\mathbf{g}_d$, which represents the non-conservative disturbing forces, in a reference part $\nabla V_{(12)E}$, modelled by the tidal potential of the Earth (E) acting on the satellites 1 and 2,

$$\nabla V_{(12)E}(\tau'; \mathbf{r}_{12}, \mathbf{r}_1; \mathbf{x_0}) = \nabla \left(V\left(\mathbf{r}_1 + \mathbf{r}_{12}\right) - V\left(\mathbf{r}_1\right)\right), \tag{9}$$

representing the long-wavelength gravity field features and in an anomalous part $\nabla T_{(12)E}$,

$$\nabla T_{(12)E}(\tau'; \mathbf{r}_{12}, \mathbf{r}_1; \Delta\mathbf{x}) = \nabla \left(T\left(\mathbf{r}_1 + \mathbf{r}_{12}\right) - T\left(\mathbf{r}_1\right)\right), \tag{10}$$

modeling the high frequent refinements and parameterized either by corrections $\Delta\mathbf{x}$ to the global gravity field parameters $\mathbf{x_0}$ or by parameters $\Delta\mathbf{x}$ of a linear approximation with space localizing base functions.

The coefficients $r_{12,\nu},\ \nu = 1, 2, ..., \infty$, of (6) can be derived by inter-satellite measurements of different types, e.g., in case of relative accelerations,

$$r_{12,\nu} = -\frac{2T^2}{\pi^2\nu^2} \int\limits_{\tau'=0}^{1} \sin\left(\nu\pi\tau'\right) \ddot{r}_{12}(\tau')\, d\tau', \tag{11}$$

and/or in case of range-rate measurements,

$$r_{12,\nu} = \frac{2T}{\pi\nu} \int\limits_{\tau'=0}^{1} \cos\left(\nu\pi\tau'\right) \dot{r}_{12}(\tau')\, d\tau', \tag{12}$$

and/or in case of inter-satellite range observations,

$$r_{12,\nu} = 2 \int\limits_{\tau'=0}^{1} \sin\left(\nu\pi\tau'\right) \left(r_{12}(\tau') - \left(1-\tau'\right) r_{12,A} - \tau' r_{12,B}\right)\, d\tau', \tag{13}$$

respectively.

There is a space domain model based on (2) with the force function according to (8) or a spectral domain model based on (7) and the spectral observations according to (11) to (13). An alternative to this approach starts with Newton's equation of relative motion as follows,

$$\ddot{\mathbf{r}}_{12}(t) = \mathbf{g}(t; \mathbf{r}_{12}, \mathbf{r}_1, \dot{\mathbf{r}}_1, \dot{\mathbf{r}}_2; \mathbf{x}). \tag{14}$$

The formulation as a boundary value problem reads, analogously to (2)

$$\mathbf{r}_{12}(t) = \left(1-\tau\right)\mathbf{r}_{12,A} + \tau\mathbf{r}_{12,B} - T^2 \int\limits_{\tau'=0}^{1} K\left(\tau,\tau'\right)\, \mathbf{g}(t; \mathbf{r}_{12}, \mathbf{r}_1, \dot{\mathbf{r}}_1, \dot{\mathbf{r}}_2; \mathbf{x})\, d\tau'. \tag{15}$$

The relative velocity can be derived by differentiation with respect to the time,

$$\dot{\mathbf{r}}_{12}(t) = \frac{1}{T}\left(\mathbf{r}_{12,B} - \mathbf{r}_{12,A}\right) - T \int\limits_{\tau'=0}^{1} \frac{dK\left(\tau,\tau'\right)}{d\tau}\, \mathbf{g}(\tau';\mathbf{r}_{12},\mathbf{r}_1,\dot{\mathbf{r}}_1,\dot{\mathbf{r}}_2;\mathbf{x})\, d\tau'. \quad (16)$$

The mathematical model for range observations can be derived by projecting the relative vector to the line-of-sight connection in combination with (15),

$$r_{12}(\tau) = \mathbf{e}_{12}(\tau) \cdot \mathbf{r}_{12}(\tau). \quad (17)$$

Analogously, the mathematical model for range-rate measurements in combination with (16) reads as follows,

$$\dot{r}_{12}(\tau) = \mathbf{e}_{12}(\tau) \cdot \dot{\mathbf{r}}_{12}(\tau). \quad (18)$$

In both equations, $\mathbf{e}_{12}$ is the unit vector in the line-of-sight direction (Fig. 1). This vector is known with high accuracy, assuming that the satellite positions are measured with an accuracy of a few cm and taking into account the distance of approximately 200km between the two satellites.

For all model alternatives the normal equations can be established and solved by a regularized solver of Tichonov type, where the regularization parameter is preferably computed according to the variance component estimation procedure of Koch and Kusche (2003).

2.2 Gravity field representation

The reference potential according to (9) can be formulated in the usual way as follows,

$$V = \frac{GM_E}{r} \sum_{n=0}^{n_{\max}} \sum_{m=0}^{n} \left(\frac{R_E}{r}\right)^n \left(c_{nm} C_{nm}(\vartheta,\lambda) + s_{nm} S_{nm}(\vartheta,\lambda)\right), \quad (19)$$

with the surface spherical harmonics,

$$C_{nm}(\vartheta,\lambda) = P_{nm}(\cos\vartheta)\cos m\lambda, \quad S_{nm}(\vartheta,\lambda) = P_{nm}(\cos\vartheta)\sin m\lambda. \quad (20)$$

The anomalous potential $T(\tau';\mathbf{r},\Delta\mathbf{x})$ according to (10) reads for a global gravity field recovery,

$$T = \frac{GM_E}{r} \sum_{n=2}^{N_{\max}} \sum_{m=0}^{n} \left(\frac{R_E}{r}\right)^n \left(\Delta c_{nm} C_{nm}(\vartheta,\lambda) + \Delta s_{nm} S_{nm}(\vartheta,\lambda)\right), \quad (21)$$

with the corrections $\Delta c_{nm}, \Delta s_{nm} \in \Delta\mathbf{x}$ to the reference potential coefficients $c_{nm},\ s_{nm} \in \mathbf{x_0}$. In case of a regional recovery the anomalous potential $T(\mathbf{r})$ is modelled by parameters of space localizing base functions,

$$T(\mathbf{r}) = \sum_{i=1}^{I} a_i \, \varphi(\mathbf{r}, \mathbf{r}_{Q_i}), \tag{22}$$

with the unknown field parameters a_i arranged in a column matrix $\Delta\mathbf{x} := (a_i,\ i = 1, ..., I)^T$ and the base functions,

$$\varphi(\mathbf{r}, \mathbf{r}_{Q_i}) = \sum_{n=0}^{N_{max}} k_n \left(\frac{R_E}{r}\right)^{n+1} P_n(\mathbf{r}, \mathbf{r}_{Q_i}). \tag{23}$$

The coefficients k_n are the difference degree variances of the gravity field spectrum to be determined minus the reference gravity field ($\Delta\bar{c}_{nm}, \Delta\bar{s}_{nm}$ are the fully normalized potential coefficients),

$$k_n = \sum_{m=0}^{n} \left(\Delta\bar{c}_{nm}^2 + \Delta\bar{s}_{nm}^2\right). \tag{24}$$

R_E is the mean equator radius of the Earth, r the distance of a field point from the geo-centre and $P_n(\mathbf{r}, \mathbf{r}_{Q_i})$ are the Legendre polynomials depending on the spherical distance between a field point P and the nodal points Q_i of the set of base functions. The maximum degree N_{max} in (23) should correspond to the envisaged maximum resolution expected for the regional recovery; in the following examples this maximum degree is selected as $N_{max} = 120$. With the definition in (23) the base functions $\varphi(\mathbf{r}, \mathbf{r}_{Q_i})$ can be interpreted as isotropic and homogeneous harmonic spline functions (Freeden et al., 1998). The nodal points are defined on a grid generated by a uniform subdivision of an icosahedron of twenty equal-area spherical triangles. In this way the global pattern of spline nodal points Q_i shows approximately uniform nodal point distances. Details can be found e.g. in Eicker et al. (2005).

3 Solution of the combined normal equations

For the analysis of GRACE observations not only the gravity field parameters have to be estimated, but also arc-related parameters as for example the two boundary position vectors of each arc. These parameters sum up to about 27000 additional unknowns for an analysis period of one month in case of short arcs with a mean arc length of approximately 30 minutes. To reduce the size of the normal equation matrices, the arc-related parameters are eliminated before the arcs are merged to the complete system of normal equations. Every short arc i builds a (reduced) partial system of normal equations $\mathbf{N}_i$. To combine the normal equation matrices for the short arcs, separate variance factors σ_i for each arc will be determined, to consider the variable precision of the range and range-rate observations. Furthermore, because of the intrinsic stability problems of the gravity field recovery process, an additional regularization factor σ_x and a regularization matrix $\mathbf{N}_x$ will be introduced into the

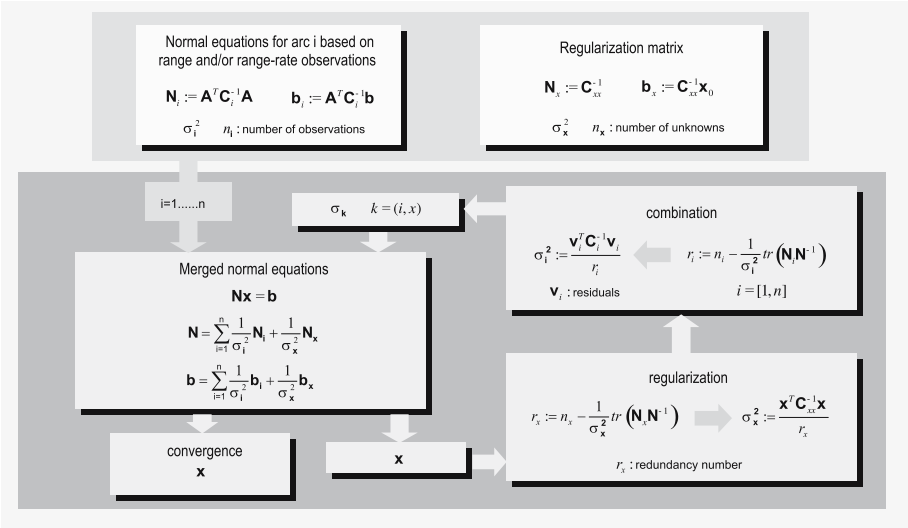

Fig. 2. Merging of normal equations for the short arcs within the iterative variance-covariance computation procedure including the determination of the regularization parameter

gravity field recovery procedure. The variance factors are computed by means of a variance component estimation procedure described by Koch and Kusche (2003). The iterative combination scheme combined with a variance component estimation and the computation of the regularization factor is shown in Fig. 2; for details of the iterative procedure refer to Mayer-Gürr et al. (2005).

4 Gravity field recovery within a simulation scenario

4.1 Simulation scenario

The recovery procedure has been tested based on a simulation scenario. It shall demonstrate the capability of the recovery approach using controlled error measures of the orbits and the inter-satellite observations. Nearly circular orbits of the GRACE twin satellites with a mean altitude of 490km and a mean distance between the two satellites of approximately 230km are generated. A pseudo real gravity field has been used for the orbit computations represented by a spherical harmonic expansion up to degree n=180. The potential coefficients have been taken over from the EGM96 gravity field model (Lemoine et al., 1998). The satellite positions are generated every 5 seconds covering a 30 days mission period. Each position coordinate is corrupted by white noise with an RMS of 3cm. Two different error scenarios for the observables have been investigated: For ***case 1***, the range-rate measurements between the twin satellites are corrupted by white noise with an RMS of

$0.2\mu m/s$ and the accelerations are considered to be measured with an accuracy of $10^{-9} m/s^2$. For ***case 2***, only the range-rate observations have been corrupted by white noise with an RMS of $1\mu m/s$, while the accelerations have been considered as error-free. For this test only range-rates have been used as observations, no ranges. The 30-days-orbit has been split into 1500 short arcs of approximately 30 minutes arc length. The total number of unknown gravity field parameters are the 19877 potential coefficients beginning from degree n=2 complete up to degree n=140. The first four potential coefficients have been fixed to one and zero, to force the centre of mass of the Earth onto the origin of the Earth-fixed reference frame. The resulting sets of potential coefficients have been truncated at degree n=110 for the subsequent comparisons with the pseudo-real solution.

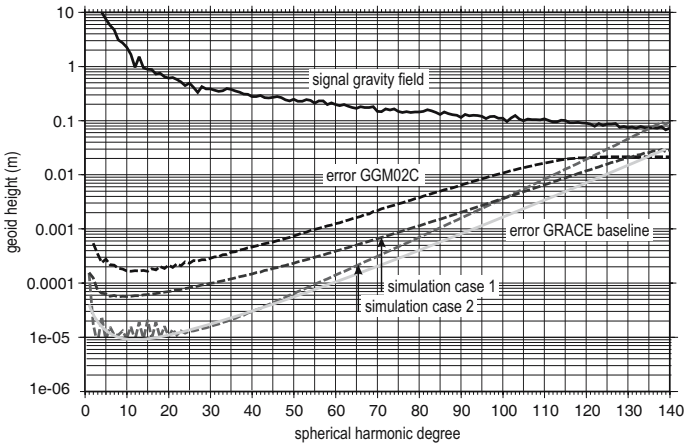

Fig. 3. Degree amplitudes of the gravity field signal, of the errors of the model GGM02C and of the errors of case 1 and case 2 as well as the expected GRACE baseline

4.2 Simulation results

The mathematical model (18) with (16) based on a spherical harmonic gravity field representation according to (8) to (10) with (19) and (21) has been applied for the gravity recovery. Fig. 3 shows the degree amplitudes of the gravity field signal, of the errors of the model GGM02C and of the errors of case 1 and case 2 as well as the expected GRACE baseline. The error degree variances of case 2 approximate the baseline quite well in the lower spectral range while the error behaviour of case 1 comes closer to the baseline in the higher frequencies. This means that the long wavelength features of the recovery result are strongly affected by the accuracy of the acceleration measurements while the effect in the higher frequencies are increasingly less

influenced. A high range-rate accuracy can be exploited only if the accelerations are known adequately. The range-rate accuracy of case 1 seems to be realistic for the GRACE mission. Therefore, one can state that the baseline has been achieved under simplified error model assumptions. It is interesting to have a closer look at the geoid differences for both cases in the space domain. Obviously, the stripe pattern of the differences to the pseudo-real solution in Color Fig. XVII on p.297 is caused mainly by the noise of the acceleration measurements, while Color Fig. XVIII on p. 297 shows the typical instability effects of the downward continuation process caused by the noise in the range-rate measurements. This holds even in case of a moderate maximum spherical harmonic degree of n=110. Nevertheless, it becomes obvious that the resolution of the recovered solution can be extended to a higher degree than the selected one (degree n=110) as Fig. 3 shows. The maximum resolution would be reached at the point where the error degree amplitude graph would intersect the signal degree amplitude graph.

5 Gravity field recovery from GRACE range-rate measurements of August 2003

5.1 Data set

The following recovery results refer to the K-band range-rate measurements of the GRACE twin satellite mission for the month August 2003. The observations are corrected for the tides caused by Sun, the Moon and the planets. The ephemerides are taken from the JPL405 data set. Effects originating from the deformation of the Earth caused by these tides are modelled following the IERS 2003 conventions. Ocean tides are computed from the FES2004 model. Effects of high frequency atmosphere and ocean mass redistributions are removed prior to the processing by the GFZ AOD dealiasing products. The 30-days-orbit has been split into 1500 short arcs of approximately 30 minutes arc length. For each arc the coordinates of the boundary vectors have been determined as well as an accelerometer bias.

5.2 Global solution

In the first step, a global spherical harmonic solution up to degree n=90 beginning from degree n=3 has been determined for the month August 2003 from the GRACE range-rate measurements, in the following designated as gravity field model “ITG-GRACE-2003-08”. The mathematical model (18) with (16) based on a pure spherical harmonic gravity field representation according to (8) and (9) with the spherical harmonic model (19) has been applied. The arc-related parameters are eliminated before merging the normal equations for each short arc to the total system of normal equations

as outlined in Sect. 3. The results are compared to the gravity field models EIGEN-CG03C (GeoForschungsZentrum Potsdam - Förste et al. 2005) and GGM02C (Centre of Space Research, Austin, - UTEX CSR, 2004, http://www.csr.utexas.edu/grace/gravity).

The geoid height differences of our model ITG-GRACE-2003-08 and the CSR model GGM02C are shown in Color Fig. XIX on p. 298: RMS: 2.6cm, avg: 2.0cm, min/max: -12.7/14.7cm. The geoid height differences with the GFZ combination model EIGEN-CG03C show similar results: RMS: 2.7cm, avg: 2.1cm, min/max: -12.4/12.5cm while the GFZ and the CSR models coincide slightly better: RMS: 2.0cm, avg: 1.6cm, min/max: -12.8/11.1cm. But one has to keep in mind that the models EIGEN-CG03C and GGM02C contain much more data covering a considerably longer mission period while our solution has been derived from only one month range-rate observations. Furthermore, the model EIGEN-CG03C has been derived as a spherical harmonic expansion up to degree n=360, including GRACE and CHAMP data as well as terrestrial gravity and altimetry data. Similarly, the CSR model has been determined as a spherical harmonic expansion up to degree n=200 from GRACE data and constrained by terrestrial data. Despite the fact that the comparisons between all these models have been performed only up to degree n=90, the quality of our model is remarkably well. In some areas such as in the Central Asian region, our solution coincides better with the model GGM02C than the model EIGEN-CG03C.

5.3 Regional solutions

For the regional refinement solutions the same mathematical model as used for the global solution and formulated in (18) with (16) has been applied except for the gravity field representation. Based upon the global solution the additional gravity field refinements are represented according to (8) with (10) represented by spherical spline functions according to (22). To avoid geographical truncation effects at the region boundaries, gravity field parameters defined in an additional strip around the specific regions have to be taken into account; the width of the strip depends on the approximation of the real field by the global reference field; in most cases a strip of 10° is sufficient. The nodal points are located at a regular grid with a mean distance between the nodal points of approximately 160km. This grid is generated by a uniform subdivision of an icosahedron of twenty spherical equal-area triangles. The regional refinement resolution corresponds approximately to the degree n=120 of a spherical harmonic representation of the residual gravity field. Fig. 4 shows the recovered gravity anomalies of the Himalayan region with its extreme rough gravity field features. A comparison with the gravity anomalies derived from the GFZ combination model EIGEN-CG03C, evaluated at a uniform grid of 1° resolution, results in an RMS of 1.32mGal, an average value of 1.06mGal and minimum/maximum differences of -5.45/5.73mGal. The corre-

sponding values with respect to the CSR model GGM02C are slightly better as follows: RMS 1.18mGal, avg 0.97mGal and min/max -3.62/4.00mGal.

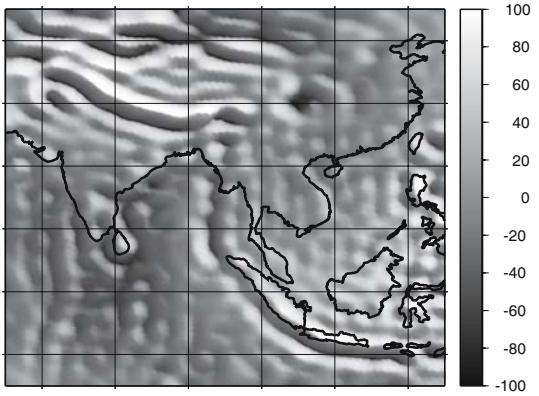

Fig. 4. Regional solution in the Himalayan area, gravity anomalies in mGal

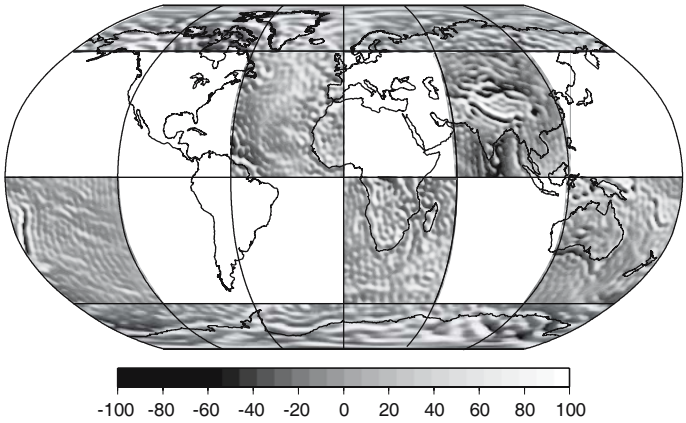

Fig. 5. Regional solution patches, gravity anomalies in mGal

5.4 Merged solutions

To combine the advantages of the satellite mission GRACE to cover almost perfectly the complete Earth with the advantages of regional focussing techniques - as pointed out earlier - the surface of the Earth has been divided into patches defined by the latitudes 60 ° and -60 °, as well as by the meridians 0 °, 60 °, 120 °, 180 °, 240 ° and 300 ° (Fig. 5). For the regional gravity field

recovery only the satellite data over the respective regions have been used. To avoid geographical truncation effects at the boundaries of the regions, an additional strip of 10 ° has been taken into account. For each patch the residual gravity field has been recovered individually applying a tailored regularization where the regularization factor as well as the variance factors for the short arcs crossing the regions are determined by a variance component estimation procedure as outlined in Sect. 3.

To derive a global gravity field model represented by spherical harmonics without losing the details of a regional zoom-in, the refined disturbing potential values are calculated at points of a specific grid, the so-called Gauss–Legendre–Grid. It has equi-angular spacing along circles of latitude; along the meridian the nodes are located at the zeros of the Legendre polynomials of degree $N + 1$. Then the potential coefficients of the spherical harmonic expansion are calculated by means of the Gauss-Legendre-Quadrature (see for example Stroud and Secrest, 1966). This quadrature method has the advantage of maintaining the orthogonality of the Legendre functions despite the discretization procedure, which allows an exact calculation of the potential coefficients,

$$\left\{ \begin{matrix} c_{nm} \\ s_{nm} \end{matrix} \right\} = \frac{R_E}{GM4\pi} \sum_{k=1}^{K} T_k P_{nm}(\cos\vartheta_k) \left\{ \begin{matrix} \cos(m\lambda_k) \\ \sin(m\lambda_k) \end{matrix} \right\} w_k, \tag{25}$$

with the area weights

$$w_k = \frac{2}{(1-t_k^2)\left(P'_{N+1}(\cos\vartheta_k)\right)^2} \quad . \tag{26}$$

The functionals T_k are the disturbing gravitational potential values at the K nodes of the quadrature, P_{nm} are the associated Legendre functions and P'_{N+1} the first derivatives of the Legendre polynomials of degree $N+1$ with respect to ϑ. N is the maximum spherical harmonic degree to be determined.

The geoid height differences of our merged model ITG-GRACE-2003-08 and the CSR model GGM02C are shown in Color Fig. XX on p. 298. The differences show an RMS of 7.27cm, an average value of 5.61cm and minimum/-maximum values of -28.7/30.6cm. The corresponding values with respect to the GFZ combination model EIGEN-CG03C (Color Fig. XXI on p. 298) are slightly worse with an RMS of 8.92cm, an average value of 6.88cm and min/-max values of -44.2/42.7cm. The GFZ and the CSR model coincide slightly better as Color Fig. XXII on p. 299 demonstrates. The RMS is 6.20cm, the average value 4.81cm and the minimum/maximum values are -35.9/36.1cm. But again, the models EIGEN-CG03C and GGM02C are not directly comparable to our one-month solution. Despite the fact that the comparisons between all these models have been performed only up to degree n=110, the quality of our model is remarkably well. In some areas is the coincidence of our solution with GGM02C better than the coincidence of GGM02C with EIGEN-CG03C, e.g., in the Central Asian region and in the polar areas.

Difference degree variances of different 2003-08-solutions with respect to the CSR gravity field model GGM02C are shown in Fig. 6 and with respect to the GFZ model EIGEN-CG03C in Fig. 7. These two gravity field models can be considered superior in quality with respect to the monthly 2003-08-solutions ITG-GRACE-2003-08, CSR-GRACE-2003-08 and GFZ-GRACE-2003-08. The difference degree variance graphs of our solution ITG-GRACE-2003-08 with respect to GGM02C and EIGEN-CG03C show slightly better results in the spectrum from degree n=70 upwards than the CSR and GFZ monthly solutions, more or less identical results in the spectral band from n=50 to 70 and still slightly worse results in the long and medium wavelength features.

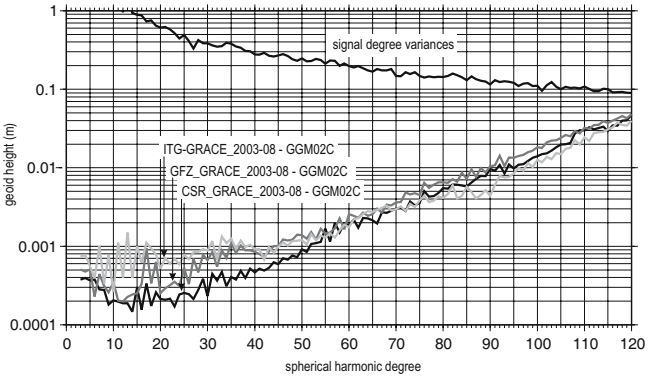

Fig. 6. Difference degree variances of different 2003-08-solutions with respect to GGM02C

This result and also the stripe pattern of the differences in Color Fig. XX and Color Fig. XXI on p. 298 could indicate some deficiencies in the bias parameter determination of the accelerometer measurements. This can be concluded from the simulation examples. Another reasons are inaccurate dealiasing products used for this analysis. But there are still numerous further reasons which have to be investigated in more details. The additional use of range measurements and the analysis of the kinematic arcs of the GRACE twin satellites may have the potential to improve the long and medium wavelength features of our recovery results.

6 Conclusions and outlook

The use of short arcs for gravity field recovery, based on the solution of Newton's equation of relative motion, formulated as a boundary value problem of Fredholm type is an adequate recovery technique for the processing of SST observations of the low-low types range and range-rates. The results achieved in

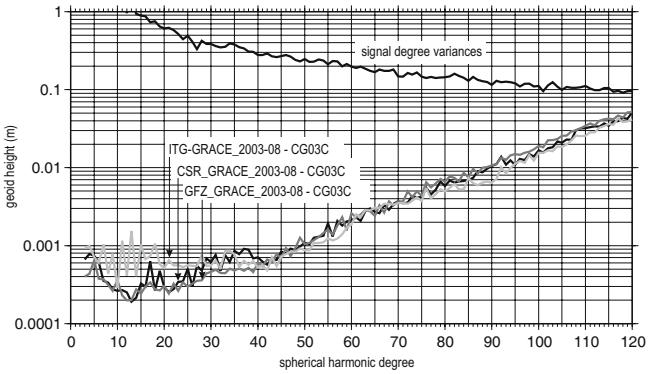

Fig. 7. Difference degree variances of different 2003-08-solutions with respect to EIGEN-CG03C

this investigation but also the successful application for the processing of kinematical arcs as an alternative to the SST high-low gravity field determination modus (cf. Mayer-Gürr et al. 2004) underline the usefulness of our gravity field recovery approach. This approach is not only very flexible in terms of various observation types of the new gravity satellite missions, moreover, it combines the advantages of a global gravity field determination with a regional gravity field zoom-in. The three computation steps a) global gravity field recovery based on a spherical harmonic expansion up to a moderate degree to provide a first global reference model as a basis for further refinements, b) regional refinements of the gravity field by spherical splines as space localizing base functions, adapted to the specific gravity field features, and c) determination of a global gravity field model by merging the regional refinement solutions and deriving potential coefficients by a numerical quadrature technique fulfil all expectations for a flexible gravity field recovery technique. Furthermore, the method is modest in terms of computation costs, as the complete global recovery problem is split up into much smaller partial problems. The computation of global gravity field models up to an arbitrary degree (only limited by the signal content of the observables) is possible on a single PC, because the stability properties of the numerical quadrature procedure do not limit the resolution to an upper degree. Together with the determination of a global solution regional zoom-ins of the gravity field are computed during the recovery procedure as well. This assures that all signal information of the observations is extracted in a best possible way.

Further improvements are expected with respect to the following aspects: a) joint use of ranges and range-rates combined with the analysis of the kinematical arcs of the GRACE twin satellites, b) refining the regularization strategy to enable smoother transition zones between the zoom-in-regions, c) tailoring the zoom-in areas more accurately to the demand of the gravity field features in the specific regions, d) more precise selection of the base functions

and the nodal point distribution adapted to the roughness of the gravity field, possibly combined with a multi-resolution strategy, e) careful investigation of the aliasing effects originating from the patching of several regional solutions, f) homogeneization of the regional solutions to avoid long wavelength errors. Besides these topics, the transformation of the mathematical model into spectral domain may enable further improvements.

Acknowledgement. We are grateful to GFZ Potsdam for providing the data for this investigation and to the Center of Space Research (Austin, USA) for providing the gravity field models. The support of BMBF (Bundesministerium für Bildung und Forschung) and DFG (Deutsche ForschungsGemeinschaft) of the GEOTECHNOLOGIEN programme is gratefully acknowledged. This is publication GEOTECH-150 of the programme GEOTECHNOLOGIEN of BMBF and DFG, Grant 03F0326C.

References

Eicker A, Mayer-Gürr T, Ilk, KH (2005) An integrated global/regional gravity field determination approach based on GOCE observations, this volume

Förste C, Flechtner F, Schmidt R, Meyer U, Stubenvoll R, Barthelmes F, Neumayer KH, Rothacher M, Reigber C, Biancale R, Bruinsma S, Lemoine JM, Raimondo JC (2005) A New High Resolution Global Gravity Field Model Derived From Combination of GRACE and CHAMP Mission and Altimetry/Gravimetry Surface Gravity Data, Poster presented at EGU General Assembly 2005, Vienna, Austria, 24-29, April 2005

Freeden W, Gervens T, Schreiner M (1998) Constructive Approximation on the Sphere, Oxford University Press, Oxford

Ilk KH (1984) On the analysis of satellite-to-satellite tracking data, Proceedings of the International Symposium on Space Techniques for Geodesy, pp. 59, Sopron

Ilk KH, Rummel R, Thalhammer M (1995) Refined Method for the Regional Recovery from GPS/SST and SGG, CIGAR III/2, ESA contract No. 10713/93/F/FL, European Space Agency

Koch KR, Kusche J (2003) Regularization of geopotential determination from satellite data by variance components, Journal of Geodesy 76(5):259-268

Lemoine FG, Kenyon SC, Factor JK, Trimmer RG, Pavlis NK, Chinn DS, Cox CM, Klosko SM, Luthcke SB, Torrence MH, Wang YM, Williamson RG, Pavlis EC, Rapp RH, Olson TR (1998) The development of the joint NASA GSFC and the National Imagery and Mapping Agency (NIMA) geopotential model EGM96, NASA/TP-1998-206861, Goddard Space Flight Center, Grenbelt, MD

Mayer-Gürr, T., Ilk, K.H., Eicker, A., (2004): ITG-CHAMP02: An Improved Gravity Field Model from a Two-Year Observation Period, New Satellite Mission Results for the Geopotential Fields und Their Variations, Proceedings Joint CHAMP/-GRACE Science Meeting, GFZ Potsdam, July 6-8

Mayer-Gürr T, Ilk, KH, Eicker A, Feuchtinger M (2005) ITG-CHAMP01: A CHAMP Gravity Field Model from Short Kinematical Arcs of a One-Year Observation Period, Journal of Geodesy (2005) 78:462-480

Reigber C (1969) Zur Bestimmung des Gravitationsfeldes der Erde aus Satellitenbeobachtungen, DGK, Reihe C, Heft Nr. 137, München

Schneider M, (1968) A General Method of Orbit Determination, Royal Aircraft Translation No. 1279, Ministry of Technology, Farnborough Hants, England

Schneider M, Reigber C (1969) On the Determination of field parameters using a generalized Fourier-Analysis, In: B. Morando (ed.) Dynamics of Satellites, Symposium Prague COSPAR - IAU - IAG/IUGG - IUTAM, Springer-Verlag Berlin 1970

Stroud AH, Secrest D (1966) Gaussian Quadrature Formulas, Prentice –Hall, Englewood Cliffs, N.J.

Tapley BD, Bettadpur S, Watkins M, Reigber Ch (2004) The gravity recovery and climate experiment: mission overview and early results. Geophys Res Lett 31, L09607: doi10.1029/2004GL019920